Testing the Model of Oscillating Magnetic Traps

Ż. Szaforz · M. Tomczak

Abstract The aim of this paper is to test the model of oscillating magnetic traps (the OMT model), proposed by Jakimiec and Tomczak (*Solar Phys.* **261**, 233, 2010). This model describes the process of excitation of quasi-periodic pulsations (QPPs) observed during solar flares. In the OMT model energetic electrons are accelerated within a triangular, cusp-like structure situated between the reconnection point and the top of a flare loop as seen in soft X-rays. We analyzed QPPs in hard X-ray light curves for 23 flares as observed by *Yohkoh*. Three independent methods were used. We also used hard X-ray images to localize magnetic traps and soft X-ray images to diagnose thermal plasmas inside the traps. We found that the majority of the observed pulsation periods correlates with the diameters of oscillating magnetic traps, as was predicted by the OMT model. We also found that the electron number density of plasma inside the magnetic traps in the time of pulsation disappearance is strongly connected with the pulsation period. We conclude that the observations are consistent with the predictions of the OMT model for the analyzed set of flares.

Keywords Energetic particles · Flares · Oscillations · Solar hard X-ray bursts

1. Introduction

One of the significant manifestations of solar flare variability are the so-called quasi-periodic pulsations (QPPs). There are nearly periodic changes of intensity in the electromagnetic radiation observed in solar-flare light curves. These changes can sometimes be observed in a wide wavelength range: from radio to γ-rays (Nakariakov *et al.*, 2010). In particular, significant oscillations are visible in wavelength ranges originating from nonthermal electrons

Ż. Szaforz (✉) · M. Tomczak
Astronomical Institute, University of Wrocław, ul. Kopernika 11, 51-622 Wrocław, Poland
e-mail: szaforz@astro.uni.wroc.pl

M. Tomczak
e-mail: tomczak@astro.uni.wroc.pl
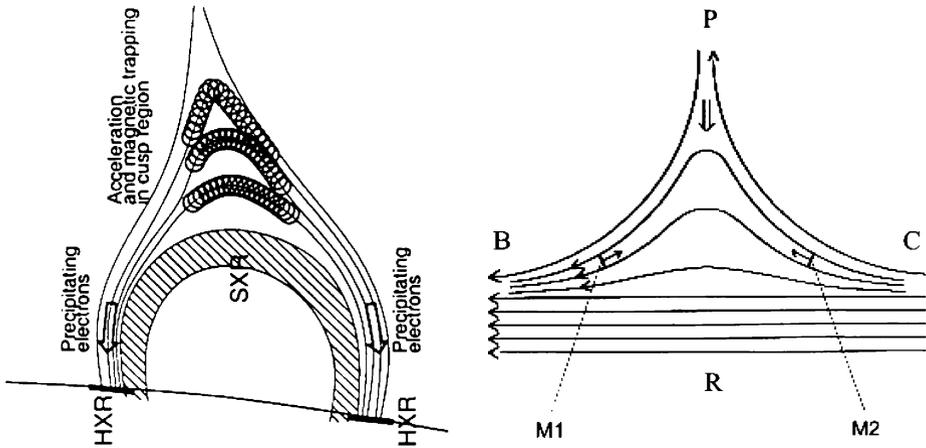
Figure 1 (a) The cusp-like structure, following Aschwanden (2004). Accelerated electrons are temporarily trapped in the magnetic trap located above soft X-ray loops. (b) Magnetic configuration in a cusp-like structure (Jakimiec and Tomczak, 2010). Magnetic field R represents the field of the SXR loop. Magnetic field lines BP and CP reconnect at P. M_1 and M_2 are the positions of magnetic mirrors.

accelerated in a flare. A wide range of periods are reported: from fractions of a second to tens of minutes. QPPs carry unique information concerning physical processes that occur in solar flares (Nakariakov and Melnikov, 2009).

Unfortunately, it has not been possible to definitively identify a particular physical mechanism responsible for QPPs. Most likely, we are dealing with several different processes. The shortest periods (subseconds), mainly observed in radio emission, are believed to be associated with the electromagnetic plasma waves or whistler waves connected with the accelerated particles (Aschwanden, 1987). Longer periods are commonly recognized as the manifestation of magnetohydrodynamic (MHD) processes in solar flaring loops or as the result of oscillatory regimes of magnetic reconnection (see the review of Nakariakov and Melnikov (2009) and references therein).

One of the interpretations for longer QPPs was proposed by Jakimiec and Tomczak (2010), who introduced the model of oscillating magnetic traps (OMT). In this model, energetic electrons are accelerated inside magnetic traps located in the cusp-like structure often seen in soft X-ray images. The cusp structure is spatially limited by the reconnection point at the top and already relaxed, circular field lines forming a magnetic loop at the bottom (Figure 1a). Interaction between the newly reconnected field lines and the loop excites MHD oscillations within the cusp-like structure.

Magnetic configuration inside a cusp-like structure is shown in Figure 1b (Jakimiec and Tomczak, 2010). Magnetic-field lines PB and PC reconnect at P. This generates a sequence of magnetic traps. Moving downward, the traps overtake each other, collide, and undergo compression. During the compression particles are accelerated within the traps. Magnetic pressure, gas pressure, and the pressure of accelerated particles increase, and finally, compression is stopped. Subsequently, the traps can expand and undergo magnetosonic oscillations. The trapping ratio decreases during the compression and reaches the lowest value at the end of the compression. Then the electrons reach the highest energies and they most easily escape from the trap towards the footpoints, where they efficiently emit hard X-ray (HXR) radiation. Electrons kept within the trap are the source of the radiation that is observed as the HXR loop-top source.

The feedback mechanism between the pressure of accelerated electrons and the amplitude of magnetic-trap oscillation is a very important matter. In the pre-impulsive phase of a flare the amplitude of pulsations is usually low. During this phase only sparse electrons fill the trap so that the number of accelerated electrons is limited. The electrons that escape the trap deposit their energy in the dense, chromospheric plasma at the footpoints, causing chromospheric evaporation. Now the chromospheric plasma fills the loop and the magnetic trap during its expansion. As a result, when the next trap is compressed, a larger amount of electrons can be accelerated and can escape from the trap. This means more efficient chromospheric evaporation and higher HXR pulses in the light curve.

In this paper, we analyze QPPs for a large number of flares to test how common the OMT model is. In Section 2 data and methods of our analysis are presented. Section 3 contains the discussion of our results in connection with the OMT model. In Section 4 we summarize our work.

2. Observations and Results

To study the periods of QPPs we used HXR light curves recorded by the *Yohkoh* Hard X-ray Telescope (HXT; Kosugi *et al.*, 1991). We used the *Yohkoh Hard X-ray Telescope Flare Catalogue* (Sato *et al.*, 2006) and selected a set of flares that had at least three distinct pulses on the HXR light curve and for which at least 10 HXT images could be reconstructed with satisfactory accuracy. To analyze plasma properties of the selected flares we used the *Yohkoh* Soft X-ray Telescope (SXT; Tsuneta *et al.*, 1991) images obtained with the Be119 and Al12 filters. Here we analyze 23 flares that satisfied our selection criteria.

2.1. Period Determination

A closer inspection of the light curve reveals that QPPs occurred simultaneously with a gradual increase in the HXR flux. We separated this smooth HXR component from the HXR pulses by a trend subtraction. We define a normalized time series $S(t)$

$$S(t) = \frac{F(t) - \hat{F}(t)}{\hat{F}(t)}, \tag{1}$$

where $F(t)$ is the measured HXR flux and $\hat{F}(t)$ is the running average of $F(t)$. The averaging time δt was determined separately for each particular flare and depended on the length of time series and the signal-to-noise ratio. The adapted values typically ranged from 20 to 40 s. Figure 2a shows the original light curve (black line) and running average (red line) for the flare of 28 June 1992. Figure 2b shows the normalized time series $S(t)$. Figures 3a and b show the same for the flare of 24 October 1991. It is clear now that the removal of the smooth component only allowed revealing pulses that were not clearly seen in the original HXR light curve.

The period of QPPs was calculated using three independent methods. In the first method we measured time intervals P_i between successive HXR peaks and calculated the period $P = \langle P_i \rangle$ and its standard deviation $\sigma(P)$. Our criterion for quasi-periodicity was $\sigma(P)/P \ll 1$. In the normalized time series $S(t)$ (Figure 2b) we can clearly see five strong pulses marked by red vertical lines. The average time interval between them was $P_1 = 56.0$ s.

Secondly, we applied the fast Fourier transform (FFT). The periodogram is shown in Figure 2c. The dominant peak represents the period $P_2 = 55.6$ s.
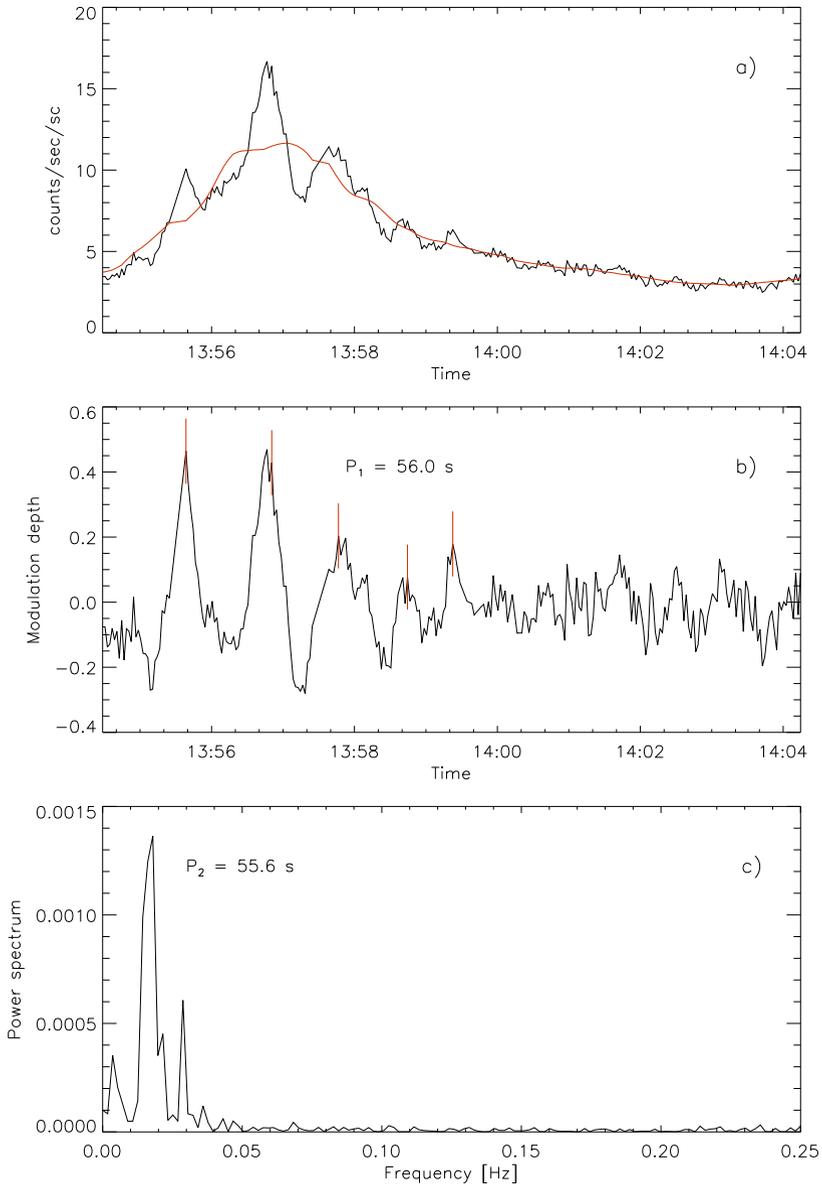
Figure 2 The flare of 28 June 1992. (a) Hard X-ray light curve recorded by *Yokoh*/HXT in the energy band M1 (23–33 keV). The red line shows the running average. (b) The normalized time series $S(t)$. The vertical red lines mark the significant maxima for which the average period, $P_1 = 56.0$ s, was calculated. (c) The power spectrum calculated for the normalized light-curve $S(t)$, with the FFT algorithm.

For the flare of 24 October 1991 the two methods gave periods $P_1 = 80.7$ s and $P_2 = 82.2$ s, respectively, which are shown in Figures 3b and c.

The last adapted method was the wavelet transform. This method has one big advantage – it gives the changes in the period as a function of time. In the top left panel of Figure 4 the
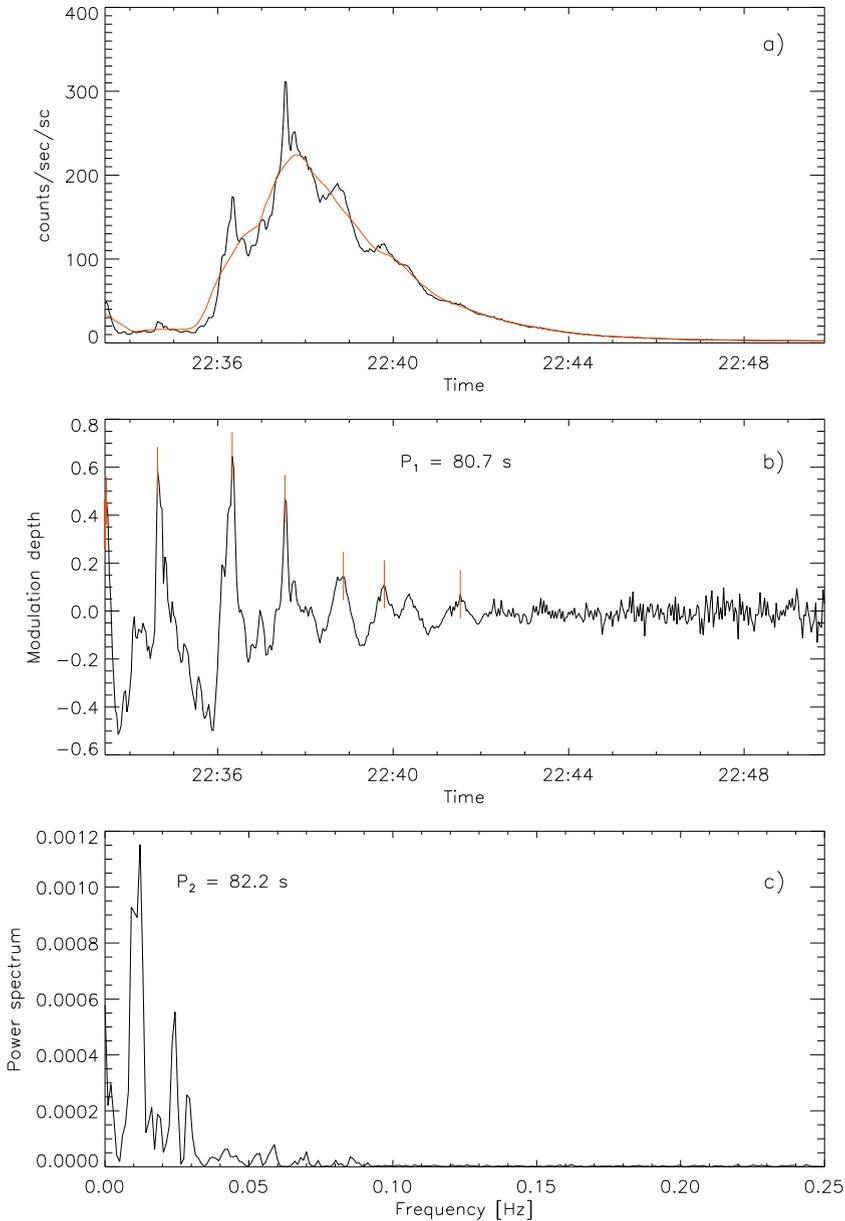
Figure 3 The same as in Figure 2 for the flare of 24 October 1991.

colors correspond to the significance of the frequency. Darker color means higher significance. The crosshatched part is called the cone of influence (COI), which marks the area that suffers from edge effects and cannot be used for period detection (Torrence and Compo, 1998). The top right panel of Figure 4 represents the global power spectrum. In this case the maximum corresponds to the period $P_3 = 60.6$ s. In the time-frequency power spec-
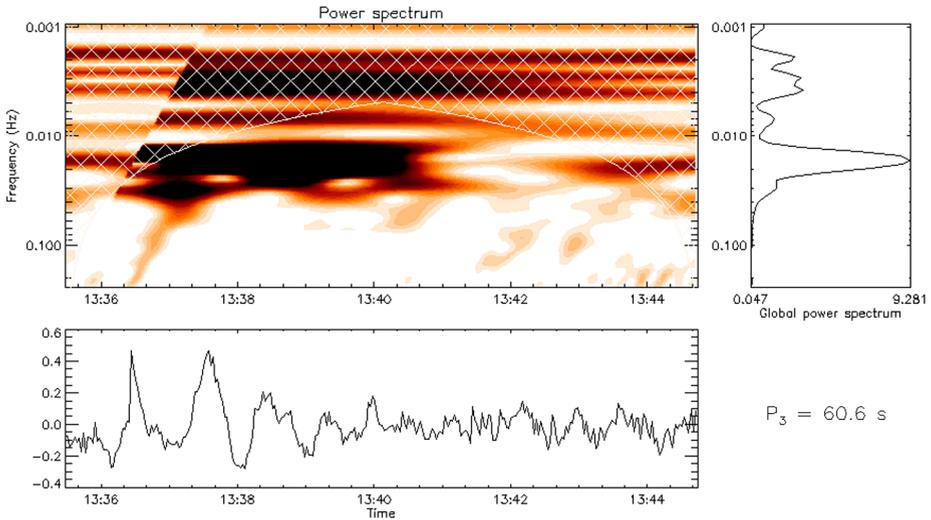
Figure 4 Top left: time-frequency power spectrum for the normalized time series $S(t)$ of the 28 June 1992 flare. The highest values of the power spectrum are shown in dark colors. The COI area is marked by white crosshatching. Top right: global power spectrum. The maximum corresponds to the period of 60.6 s. Bottom: normalized light-curve, $S(t)$.

trum (lower panel of Figure 4) the pulse disappearance time is clearly seen, just before 14:00 UT.

In Table 1 the results for 23 flares observed by *Yohkoh* are presented. The periods obtained with all the three methods are usually quite similar. The average scatter of the results is approximately 3 % of the average period. In some cases more than one significant period was detected. In some cases only one or two of the three methods detected the second period.

2.2. Imaging of Magnetic Traps

In the next step the shape of the loop-top HXR source was determined. We used the maximum-entropy method to reconstruct HXT images for all flares. This method proved to be stable and relatively fast, which is very important for reconstructing a large number of images. We used time intervals between consecutive Be119 images as the time of accumulation. This allowed us to link the reconstructed HXR images with associated SXR images. We defined the loop-top HXR source in individual image as a set of pixels within the contour of 50 % of the flux of the brightest pixel in the image. In Figure 5 a sequence of images for the 28 June 1992 flare is presented. The flare was a large arcade of loops situated exactly on the western solar limb. The impulsive phase of this flare was described by Tomczak (1997). The HXR 50 % contour levels are marked with the white thick line. For comparison, the flare of 24 October 1991 was observed as a single, compact loop on the solar disk (Figure 6).

For each flare we determined the resulting HXR source. For each individual image we created a matrix with the value 1 corresponding to the position of pixel within the 50 % contour and 0 outside the contour. We added these matrices and determined the resultant HXR source as a collection of pixels that occurred in at least half of all the reconstructed images.

Table 1 List of 23 solar flares for which periods of QPPs were determined by using the following methods: the average time interval between successive maxima of HXR bursts (P_1), the fast Fourier transform (P_2), and the wavelet transform (P_3). N_e is the electron number density at the time of pulsation disappearance.

No.	Date (dd/mm/yy), time [UT]	P_1 [s]	P_2 [s]	P_3 [s]	$n_e \times 10^{10}$ [cm^{-3}]
1	24/10/91 22:33 – 22:50	80.7	82.2	85.7	11
2	31/10/91 09:08 – 09:13	35.3	65.0, 26.0	55.6	7.1
3	10/11/91 20:05 – 20:12	108.0	112.0, 37.5	102.0, 36.0	
4	17/11/91 18:33 – 18:37	55.0, 21.5	23.5	25.5	36
5	18/12/91 10:27 – 10:33	62.0	57.8	60.6	16
6a	06/02/92 03:16 – 03:21	81.0, 30.0	78.0, 29.5	85.7, 29.0	
6b	06/02/92 03:21 – 03:37	88.4	92.4, 57.8	93.5, 55.0	
7	28/06/92 13:54 – 14:04	56.0	55.6	60.6	2.3
8	20/08/92 09:03 – 09:28	38.8	39.4	39.3	1.9
9	06/09/92 06:54 – 07:03	44.0	42.1	42.9	14
10	05/10/92 09:24 – 09:31	68.0, 39.0	65.0, 39.0	72.1	
11	22/11/92 23:07 – 23:13	42.0, 20.7	27.4	25.5	28
12	25/06/93 03:14 – 03:30	56.3, 92.0	87.3, 56.5	93.5	16
13	27/09/93 12:07 – 12:17	101.0	114.8, 52.2	121.3	26
14	16/01/94 23:11 – 23:21	46.5	46.0	51.0	11.85
15	29/01/94 11:20 – 11:32	130.0, 28.0	140.8	121.3	74
16	06/05/98 08:02 – 08:15	35.9	38.1	36.0, 132.2	9.6
17	08/05/98 01:57 – 02:18	69.2	72.7	157.3, 72.1	6.1
18	28/05/98 19:02 – 19:11	46.8	49.5	51.0	6.3
19	18/08/98 08:18 – 08:31	59.3, 158.0	154.8	144.2	42
20	07/03/00 19:46 – 19:53	23.0, 59.3	60.0, 28.0	66.1, 25.0	6.5
21	23/06/00 22:14 – 22:31	64.0, 35.3	53.6	55.6	5.0
22	24/11/00 15:08 – 15:19	46.0	50.0	51.0	18
23	05/04/01 08:30 – 08:49	89.0	94.7, 36.6	93.5, 33.0	
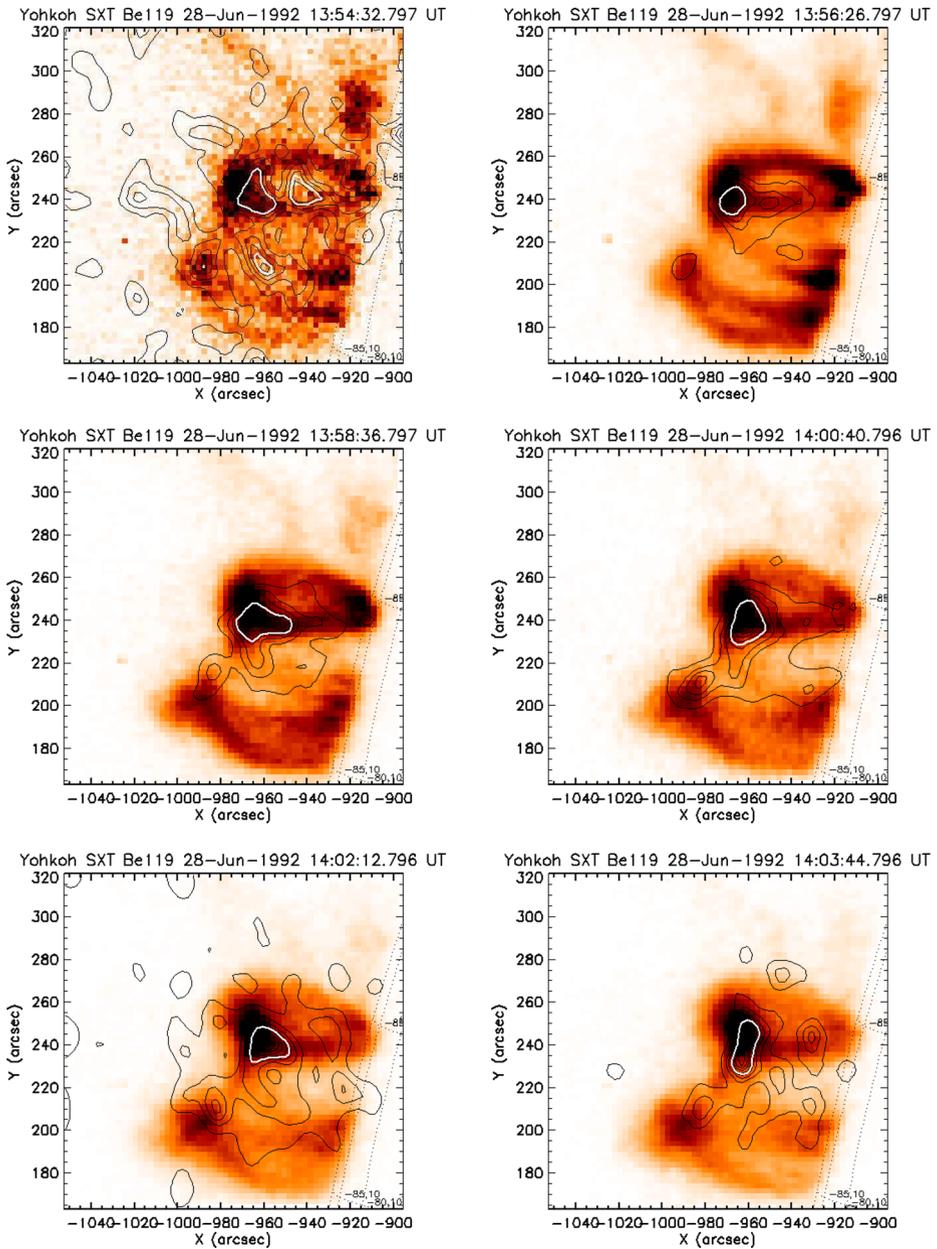
Figure 5 The sequence of SXT Be 119 images, showing the time evolution of the 28 June 1992 flare. The contour levels represent the HXT M1 intensities. The HXR top source is marked by the white thick line.

The errors of the resulting HXR source dimension should be dominated by the influence of the selected contour level that determines the source. We checked how changes of this level influence the dimension. We calculated the size of the source assuming contour levels
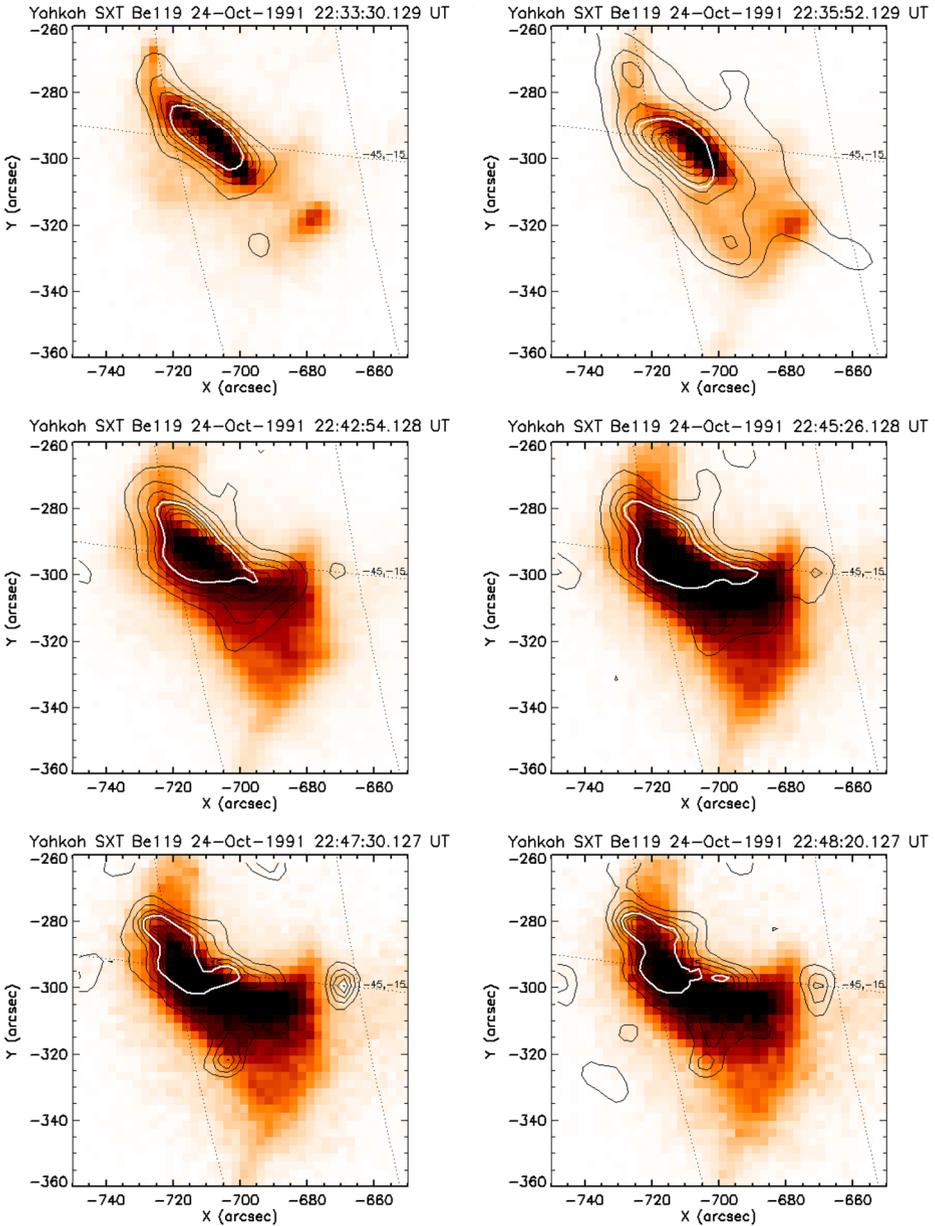
Figure 6 The same as in Figure 5 for the flare of 24 October 1991.

of 40 % and 60 %. As a measure of the dispersion we took the difference between the sizes
of the source for these two levels. The average difference is about 2.4 Mm.

We determined properties of the thermal plasma inside a loop-top HXR source as follows:
We calculated the temperature and emission measure (EM) from the SXT Be119 and Al12

filter ratios. The electron number density was calculated from the formula

$$N_{\rm e} = \sqrt{{\rm EM}/V}, \tag{2}$$

where V is the volume of the HXR source. To obtain this volume an estimation of thickness of a source along the line-of-sight is needed. We assumed it as the smaller size of the HXR source multiplied by a correction factor 1.15 (Bąk-Stęślicka and Jakimiec, 2005). Bąk-Stęślicka (2007) compared the values of electron number density obtained by two methods for a set of 40 flares: by using Equation (2) with the mentioned correction factor, and by applying the scaling law proposed by Rosner, Tucker, and Vaiana (1978). The ratio of these values was in the range $0.75 – 1.25$. We can therefore estimate that the electron density obtained by us is vitiated by an error of about 25 %.

Time variations of the temperature, the emission measure, the electron number density, and the number of pixels within the loop-top source for the 28 June 1992 flare are presented in Figure 7. The scatter seen in all the panels is caused mainly by changes in the shape of the HXR loop-top source, which is a consequence of HXT image deconvolution. Therefore it is hard to determine to what extent our reconstructed images depict the actual source. We used accumulated values for individual flares obtained for pixels that were within the loop-top sources for a majority of synthesized images to limit the influence of the deconvolution process in Section 3.

3. Discussion

The OMT model predicts that the period of oscillation P and the size of the magnetic trap d are correlated. According to this model, the length of a magnetic trap should be equal to the larger size of the loop-top HXR source. In Figure 8 the black symbols are taken from Jakimiec and Tomczak (2010) and support the close relationship between d and P. The red stars correspond to the flares from Table 1. A similar correlation between the periods and the trap diameters is clearly seen. We also obtained the second branch in the $P–d$ diagram, which is revealed by the blue triangles. They are introduced by the events for which the second, longer period was detected. The origin of periodicity from the second branch is still unclear. It is possible that there were some larger loops involved, which contributed somewhat to the observed emission, but the sources of the flares were too weak (or too high) to be seen in the HXR images. In two cases we can interpret the second period as the oscillations of the entire flaring loop (Zaitsev and Stepanov, 1982). If we assume the magnetic-trap dimension as the size of the whole loop, the points corresponding to these two flares will move up in the $P–d$ diagram (purple triangles with arrows).

The pulses disappear when the density inside the trap becomes too high (Jakimiec and Tomczak, 2012). In this case the accelerated electrons are quickly thermalized within the loop-top structure. Jakimiec and Tomczak (2012) estimated this density to be around 9×10^{10} cm^{-3}. We investigated the time changes in electron number density within the HXR loop-top sources and found that, indeed, there usually is a termination value for which the HXR pulses disappear. The obtained values were in a broad range from 1.9×10^{10} to 7.4×10^{11} cm^{-3}. Our results suggest that there is a correlation between the period of QPPs (and thus also between the diameter of a trap) and the electron number density at the time of pulsation disappearance. Figure 9 shows this relation for 19 flares for which the time of pulsation disappearance was clearly observed in the HXR light curves. The correlation coefficient is $R = 0.67$. This relation means that the larger the magnetic trap, the higher the electron number density values reached before the thermalization rate exceeds the rate of electron acceleration.
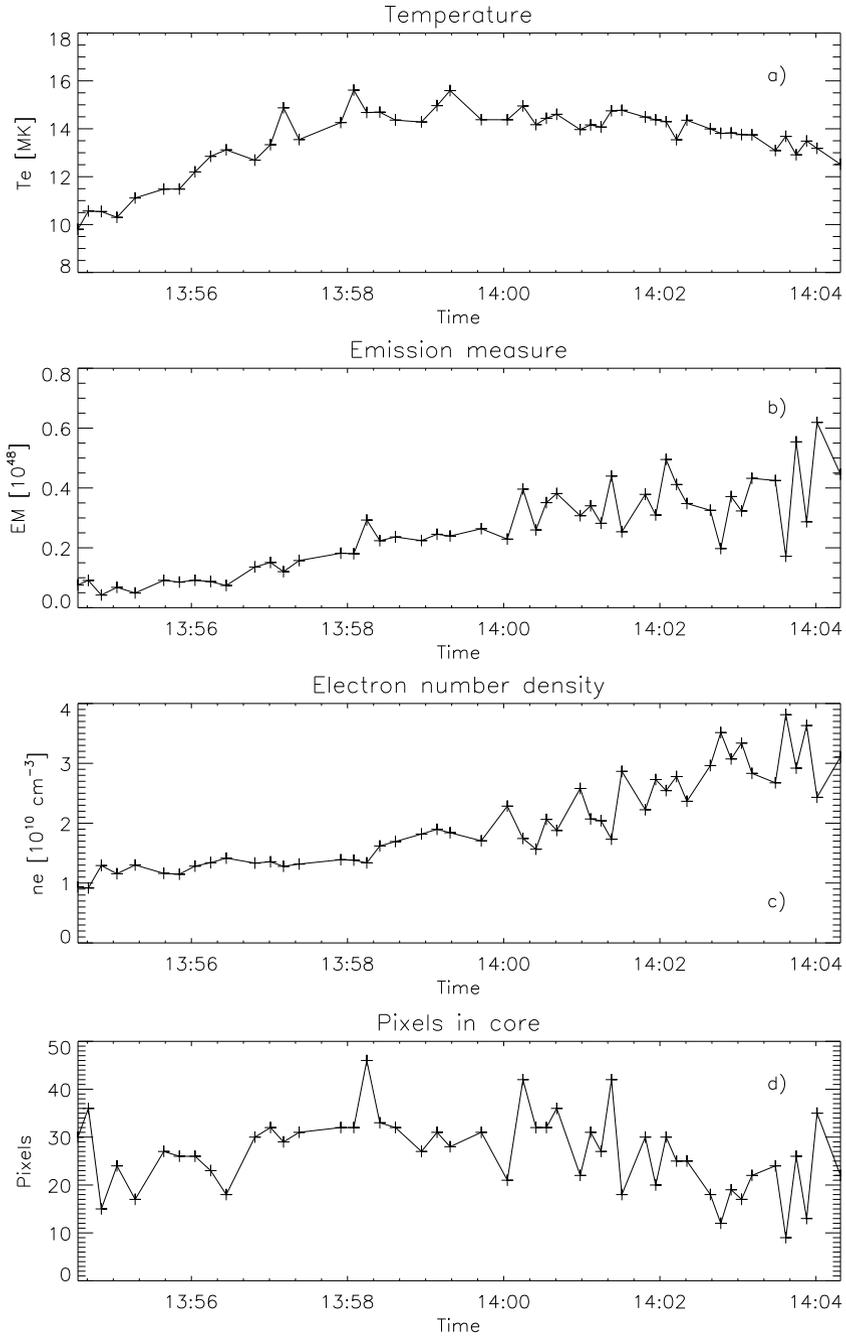
Figure 7 Time variations of the HXR loop-top source plasma parameters obtained from the SXT Be 119 and Al12 filter ratios: (a) the temperature, (b) the emission measure, (c) the electron number density, and (d) the number of pixels within the loop-top source.
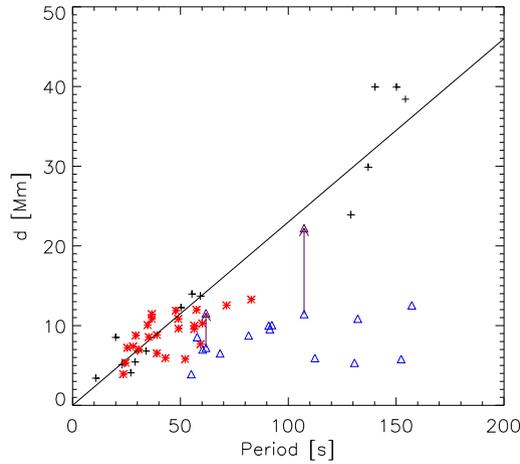
Figure 8 Correlation between the HXR loop-top source diameter, d, and the oscillation period, P. Black symbols correspond to flares analyzed by Jakimiec and Tomczak (2010). They obtained a correlation equation $d = (0.0 \pm 1.3) + (0.23 \pm 0.03) \times P$. Red symbols correspond to the flares from Table 1. When the second period was excited, we obtained the second set of points marked as blue triangles. In two cases we can interpret the second period as the oscillations of the entire flaring loop (Zaitsev and Stepanov, 1982). These situations are shown as arrows and purple triangles.

Figure 9 Correlation between the electron number density in the time of pulsation disappearance and the period of the QPPs. Periods obtained by first method, *i.e.* by measured time intervals P_i between successive HXR peaks and calculated the period $P = \langle P_i \rangle$, were used. In the cases when two period was obtained more significant period was used.
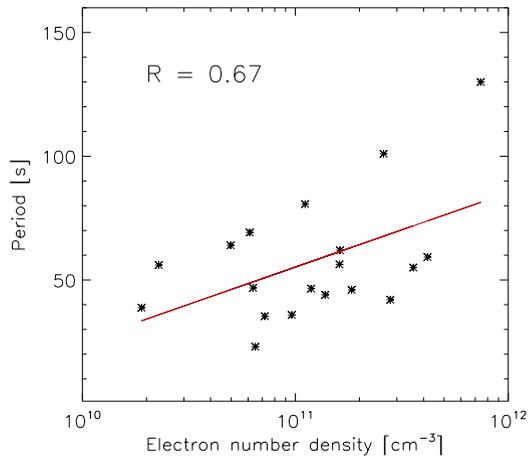
4. Summary

We have investigated a set of flares recorded by the *Yohkoh* satellite for which quasi-periodic variations of hard X-ray flux were clearly seen. We determined the pulsation periods using three independent methods. We also estimated the values of parameters of the hot thermal plasma inside the loop-top HXR sources. We used these data to test the OMT model proposed by Jakimiec and Tomczak (2010).

The amplitudes of QPPs change in time. Weak pulses usually occur at the beginning of a flare. During the impulsive phase, the pulsation amplitude increases significantly. The OMT model predicts that during the compression of a trap the particles are accelerated, while

during its expansion a plasma derived from chromospheric evaporation fills the trap. This is the reason why during the next compression of the trap more electrons can be accelerated, and the amplitude of pulsation increases. This feedback works as long as the electron number density is low enough to allow electrons to leave the trap before their thermalization. The termination value probably depends to some degree on local conditions. We have found the correlation between the period of QPPs and the electron number density at the time of the pulsation disappearance.

Our analysis confirmed the correlation between the size of the HXR loop-top source and the pulsation period. Furthermore, we found that some flares reveal a second oscillation period. We propose that this period is connected with some larger magnetic structures that not seen in HXR images, but are clearly visible in SXR and EUV images. This requires a more detailed comprehensive analysis.

We conclude that the OMT model adequately describes the HXR observations of many flares.

References

Aschwanden, M.J.: 1987, Theory of radio pulsations in coronal loops. *Solar Phys.* **111**, 113.

Aschwanden, M.J.: 2004, *Physics of the Solar Corona. An Introduction*, Springer, Berlin.

Bąk-Stęślicka, U.: 2007, Investigation of evolution of solar flares. Ph.D.thesis, University of Wroclaw (in Polish).

Bąk-Stęślicka, U., Jakimiec, J.: 2005, Investigation of X-ray flares with long rising phases. *Solar Phys.* **231**, 95.

Jakimiec, J., Tomczak, M.: 2010, Investigation of quasi-periodic variations in hard X-rays of solar flares. *Solar Phys.* **261**, 233.

Jakimiec, J., Tomczak, M.: 2012, Investigation of quasi-periodic variations in hard X-rays of solar flares. II. Further investigation of oscillating magnetic traps. *Solar Phys.* **278**, 393.

Kosugi, T., Makishima, K., Murakami, T., Sakao, T., Dotani, T., Inda, M., *et al.*: 1991, The Hard X-ray Telescope (HXT) for the SOLAR-A mission. *Solar Phys.* **136**, 17.

Nakariakov, V.M., Melnikov, V.F.: 2009, Quasi-periodic pulsations in solar flares. *Space Sci. Rev.* **149**, 119.

Nakariakov, V.M., Inglis, A.R., Zimovets, I.V., Foullon, C., Verwichte, E., Sych, R., Myagkova, I.N.: 2010, Oscillatory processes in solar flares. *Plasma Phys. Control. Fusion* **52**, 124009.

Rosner, R., Tucker, W.H., Vaiana, G.S.: 1978, Dynamics of the quiescent solar corona. *Astrophys. J.* **220**, 643.

Sato, J., Matsumoto, Y., Yoshimura, K., Kubo, S., Kotoku, J., Masuda, S., *et al.*: 2006, YOHKOH/WBS recalibration and a comprehensive catalogue of solar flares observed by YOHKOH SXT, HXT and WBS instruments. *Solar Phys.* **236**, 351.

Tomczak, M.: 1997, The impulsive phase of the arcade flare of 28 June 1992, 14:24 UT. *Astron. Astrophys.* **317**, 223.

Torrence, C., Compo, G.P.: 1998, A practical guide to wavelet analysis. *Bull. Am. Meteorol. Soc.* **79**, 61.

Tsuneta, S., Acton, L., Bruner, M., Lemen, J., Brown, W., Caravalho, R., *et al.*: 1991, The Soft X-ray Telescope (SXT) for the SOLAR-A mission. *Solar Phys.* **136**, 37.

Zaitsev, V.V., Stepanov, A.V.: 1982, On the origin of the hard X-ray pulsations during solar flares. *Sov. Astron. Lett.* **8**, 132.